Design of the Ciervana Breakwater

Burcharth, Hans Falk; Frigaard, Peter Bak; Uzcanga, J.; Berenguer, J. M.; Madrigal, B. G.; Villanueva, J

Published in:
Conference on Coastal Structure and Breakwater

Publication date:
1995

Document Version
Early version, also known as pre-print

Design of the Ciervana breakwater, Bilbao

Hans F. Burcharth and Peter Frigaard
Hydraulics Laboratory, Aalborg University

Javier Uzcanga
Autoridad Portuaria de Bilbao

José Maria Berenguer and Braulio Gonzalez Madrigal
Centro de Estudios de Puertos y Costas
of CEDEX

Jesus Villanuera
Autoridad Portuaria de Bilbao

ABSTRACT

A major expansion of Port of Bilbao includes some 4.5 km of breakwaters in water depths up to 28 metres. Construction costs is approximately 190 mill. USD. The paper presents the lay-out and the cross section of the most exposed breakwater section. Further is described the environmental design conditions, the design wave climate, the hydraulic model tests for investigation of toe berm and armour stability as well as forces on the parapet wall and the overtopping. Model tests were performed in 1989-90 at the Hydraulics Laboratory, Aalborg University, Denmark and at Centre for Studies and Experiments in Ports and Coasts, CEDEX, Madrid. A comparison between results from the two laboratories is presented.

LAY-OUT OF THE PORT EXPANSION

Bilbao is situated on the north coast of Spain at the mouth of the river Nervión, which faces the Bay of Biscaya. Milestones in the history of the Port of Bilbao are:

- Year 1900, where the channelling of the river began and breakwaters and quays were built in water depths up to 14 metres in the inner part of the bay called the Abra.
- Year 1970, where the installation of an oil refinery in Bilbao necessitated the building of the 2.5 km long breakwater at Punta Lucero in water depths of up to 32 metres in the outer part of the Abra in order to provide shelter for tanker berths up to 500.000 DWT.
- Year 1976, where the Punta Lucero breakwater was completed.
- Between 1980 and 1985 the Punta Lucero breakwater was reinforced considerably after suffering severe damage during storms in 1976. The original armour layer of 85 t parallelepiped blocks were covered with 150 t blocks, the width and mass of the parapet wall were increased considerably and the rear slope expanded and armoured with 20 t blocks in the upper part.

The need for more space on land to support further development of the port led to the present project for a major expansion of the part in the bay between the inner port and the Punta Lucero breakwater, see Fig. 1.

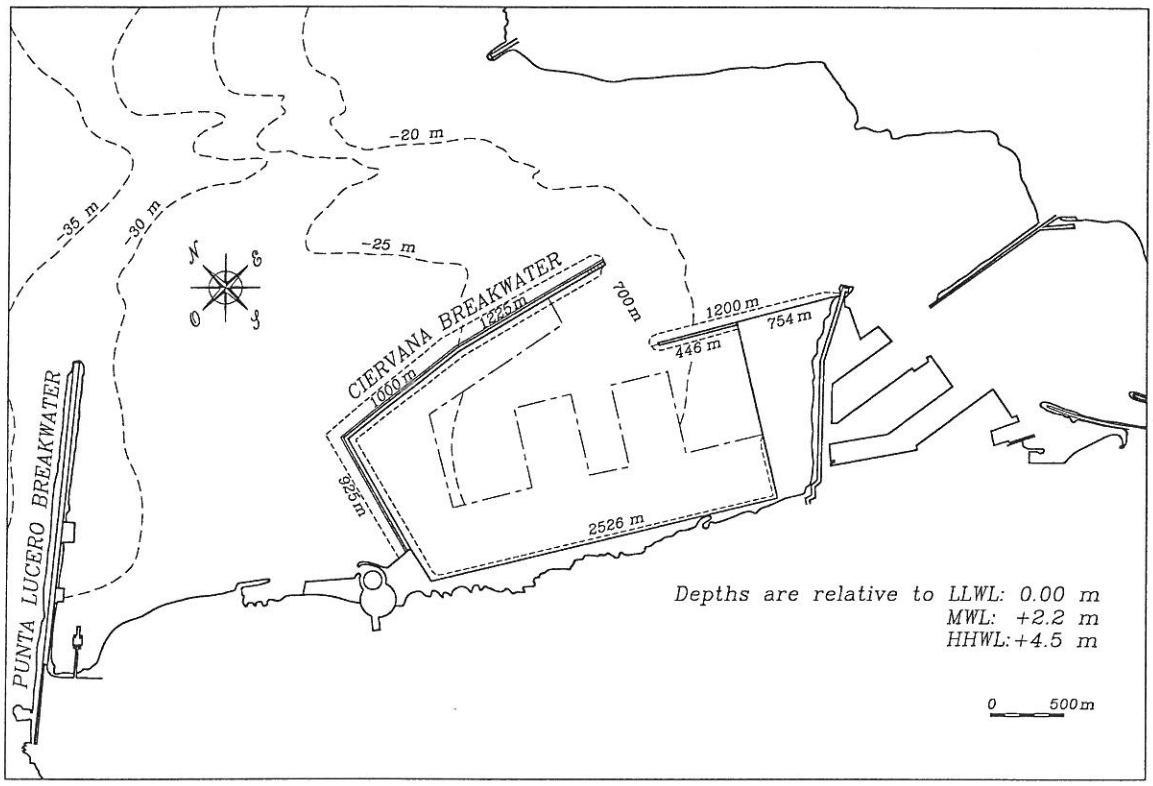

Fig. 1. Lay-out of the Port of Bilbao expansion.

The outer main breakwater, named the Ciervana breakwater after the village at its landing, is 3.15 km long. The secondary breakwater south of the 700 m harbour entrance has a length of 1.20 km. An important factor influencing the lay-out of the Ciervana breakwater with its pronounced 80 degrees bend was the need for limiting wave reflection into the tanker berth area at the south side of the Punta Lucero breakwater. A rubble mound structure was preferred for the same reason. The lay-out of the port expansion was decided on the basis of numerical models for wave disturbance (model of Prof. Sánchez Arcilla operated by Port of Bilbao Technical Services and the S21 model of Danish Hydraulic Institute operated by Centro de Estudios de Puertos y Coastas of CEDEX). Further a three-dimensional physical model to scale 1:150 at CEPYC was used for final check on wave disturbance and movements of moored vessels. Manoeuvring conditions for the vessels were studied in a numerical ship simulator by Delft Hydraulics.

The first phase of the project comprises the breakwaters, a 850 m long caisson structure quay at 21 metres water depth and 425,000 m^2 of reclaimed land.

OFFSHORE WAVE CLIMATE

An extreme statistics for offshore storm waves of different directions of propagation was estimated by Prof. Y. Goda, mainly based on 13 years (1976-1988) of scalar Waverider buoy records located just outside the bay in 30 m and 50 m water depths, visual wave data for the Bay of Biscay for the period 1950-1985 provided by National Climatic Data Center of the US Navy, Ashville, and hindcast of larger storms in the period 1955-1981 provided by the Danish Hydraulic Institute.

Only larger storms with offshore wave directions within the sectors NW, NNW, N can have significant impact on the breakwaters. Table 1 gives the central estimate of return period of max significant wave heights $\hat{H}_s$ within single storms and the estimated standard deviations σ covering the statistical uncertainty due to limited data and an empirically determined uncertainty due to unknown true distribution.

Table 1. Estimated long term "offshore" wave climate at bay entrance in 30 m water depth.

	central estimates all directions		10% exceedence probability estimates NW	NNW	N
Return period (year)	$\hat{H}_s$ (m)	σ (m)	H_s	H_s	H_s
1	6.4	0.5	6.7	6.0	5.0
10	8.3	0.6	8.6	7.7	6.4
50	9.5	0.9	10.1	9.0	7.5
100	10.0	1.0	10.7	9.6	7.9
200	10.5	1.2	11.4	10.7	8.4
500	11.1	1.4	12.3	11.0	9.0

DESIGN CONDITIONS

As basis for the design wave climate in front of the structure was applied the 10% exceedence probability estimates on the offshore $\hat{H}_s$ values (Table 1). The refraction and diffraction coefficients were determined from the above mentioned physical and numerical models. The design wave climate along the most exposed part of the main breakwater is shown in Fig. 2 for return periods 1, 200 and 500 years.

Offshore wave directions NW and NNW caused almost the same angle of incidence at the breakwater. As the response of the structure is not sensitive to small variations in wave direction it was decided to merge the two directions into one mean direction, shown as 30° degrees in Fig. 2, in order to reduce the model test program, which anyway was comprehensive due to the large variations in wave climate along the structure and due to the corners. In the major part of the model tests the angle of incidence was reduced to 20° because the smaller obliqueness turned out to be more dangerous.

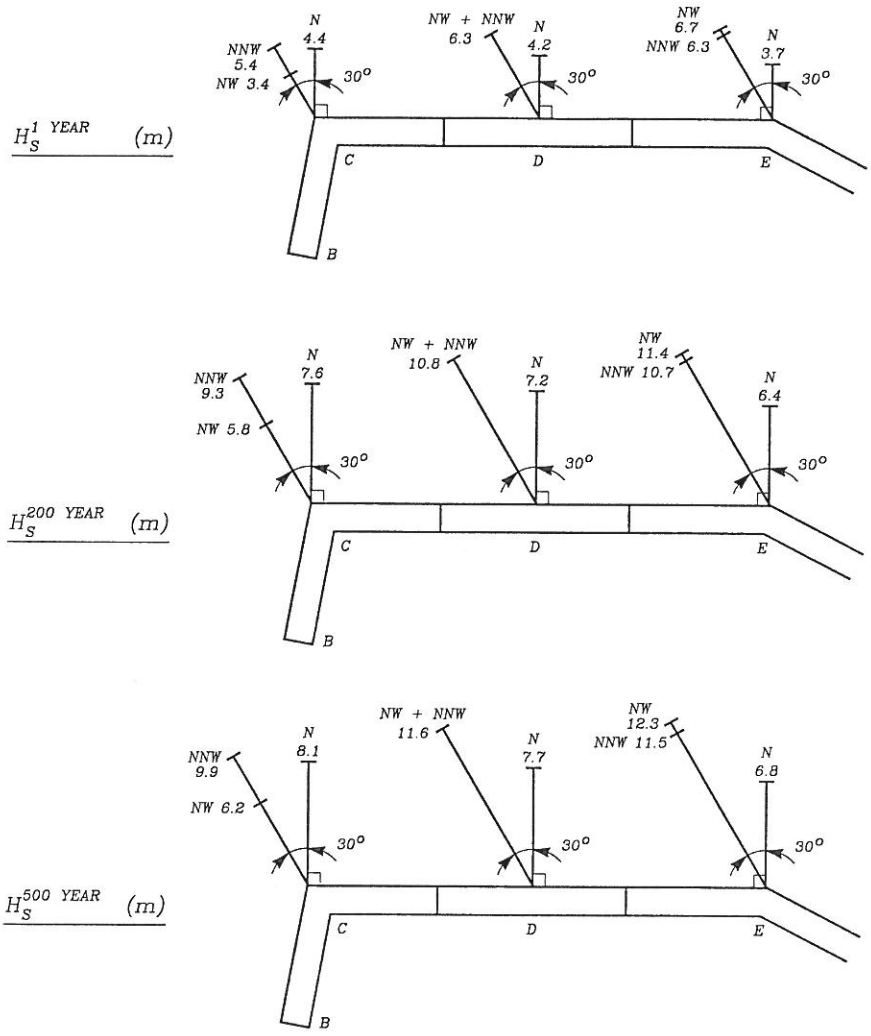

Fig. 2. Design wave climate along the outer breakwater given as 10% exceedence probability estimates on $\hat{H}_s$. The given directions N, NNW and W refer to the offshore wave directions. The directions given by the vectors refer to the wave direction just in front of the breakwater.

For the structural safety and overtopping the following rather conservative "design criteria" were applied:

Wave wall : No damage for sea states corresponding to an exceedence level of 20% in 100 years structure life (equivalent encounter probability return period of 500 years).

This conservative criterion is due to the large costs involved in case of damage.

Main armour : Moderate damage (max 15% displaced blocks but no exposure of the filter layers in front of the wave wall) for the same sea state as mentioned for the wave wall.

Little damage (max 5-10% displaced blocks) which do not need immediate repair for sea states corresponding to an exceedence level of 40% in 100 years structural life (equivalent encounter probability return period of 200 years).

Overtopping : Mean value of 10^{-4} $m^3/m/sec$ for the 1 year return period sea state.

Mean value of $2 \cdot 10^{-3}$ $m^3/m/sec$ for the 50-100 year return period sea state.

The choice of these low figures, which correspond to safe passage of persons and vehicles, is due to the future use of reclaimed areas behind the breakwater.

BREAKWATER CROSS SECTIONS

Fig. 3. shows the final cross section of the most exposed section of the outer breakwater.

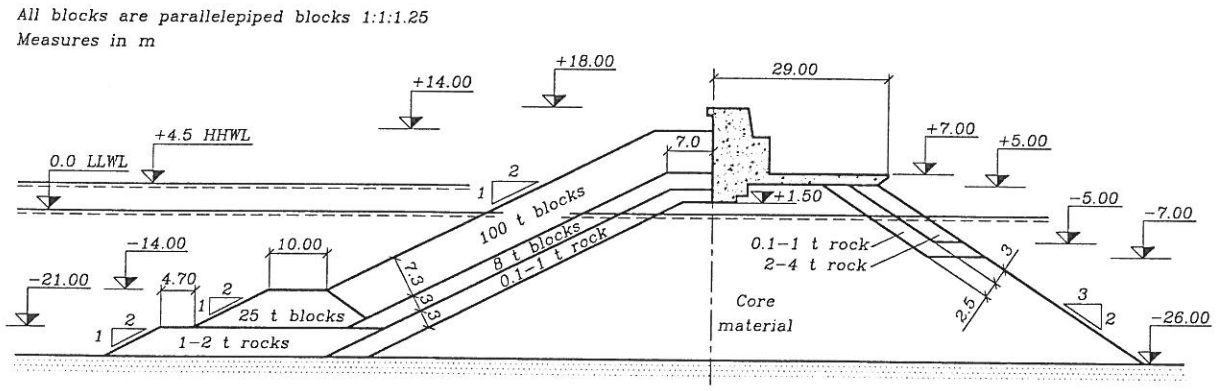

Fig. 3. Typical cross section of the outer breakwater.

The main armour, the secondary armour and the toe berm consist of parallellepiped unreinforced concrete blocks of side length ratios 1 to 1 to 1.25. The prototype mass density of the concrete and the rocks are $2.30\,t/m^3$ and $2.65\,t/m^3$, respectively.

MODEL TESTS

Introduction

The cross sections were optimized on the basis of model tests performed at the Hydraulics Laboratory, Aalborg University, AU, and at CEPYC of CEDEX, Madrid.

The main elements in the study were:

- toe berm and main armour stability including influence of block placement methods
- wave forces on parapet walls
- overtopping (mean discharge)

AU studied the corner section including trunk sections in oblique and head-on waves. Moreover, the stability of the rear slope armour was tested at AU. CEDEX studied trunk sections in oblique and head-on waves. Due to the overlap with respect to trunk sections a comparison between results from the two laboratories was possible. The observed discrepancies which are discussed below might be due to differences in model set-up and wave generation techniques.

Waves

Both laboratories applied long crested irregular waves in accordance with the JONSWAP spectrum with peak enhancement factors $\gamma = 1.4$ and 4.0. The same sea state histories as given in Table 2 were applied in the two laboratories.

Table 2. Model test sea state histories (prototype figures).

H_s (m)	7	8	9	10	11	12	13
T_p (sec)	13, 15	13, 15	15, 17	15, 17	15, 17, 19	17, 20	17,20

The range of the Irribarren number $Ir = tan\alpha \left(H_s/L_o^{T_p}\right)^{-0.5}$ is 2.8 - 3.6.

At AU the duration of each step corresponded to app. 9.3 hours in prototype of randomly generated waves with no repetitions (2,100 - 3,300 waves).

At CEDEX the duration of each step corresponded to app. 7.8 hours, i.e. app. 20% less than at AU. Moreover, each step was made up of 5 identical sequences of app. 300 - 400 waves.

Other differences related to the applied wave generation at the two laboratories are as follows: At AU the waves were generated in a 10 m wide tank with a piston-type wave paddle in water depth corresponding to 34.2 m at HHWL and the sea bed slope was 1 : 60 reaching a water depth of 30.5 m at the model. The length scale was 1 : 87. At CEDEX the waves were generated in a 6.5 m wide tank with a bottom hinged paddle in water depth corresponding to 85.5 m and the sea bed profile in front of the model was broken with two sloping sections (20% and 14%) in between horizontal plateaus of which the latter corresponded to a water depth of 30.5 m at the model. The length scale was 1 : 60. It follows that the shoaling of the waves in the two laboratories were different, which again introduces differences in the kinematics of the waves in front of the model. However, such differences could not be seen in the surface elevation variance spectra, but will probably influence the impact on the model and the response.

The wave height distribution in the AU tests was checked against shallow water prototype data (Stive 1986) given by

$$\hat{H}_{1\%} = H_{mo}(0.5\,ln\,100)^{0,5}(1 + H_{mo}/d)^{-0.33}$$
$$\hat{H}_{0.1\%} = H_{mo}(0.5\,ln\,1000)^{0,5}(1 + H_{mo}/d)^{-0.5}$$

where d is the water depth. $\hat{H}_{n\%}$ is the $n\%$ exceedence value of wave height determined by zero crossing analysis and $H_{mo} = 4\sqrt{m_o}$, where m_o is the zero spectral moment. Fig. 4 shows a typical comparison. Generally very good agreement was found.

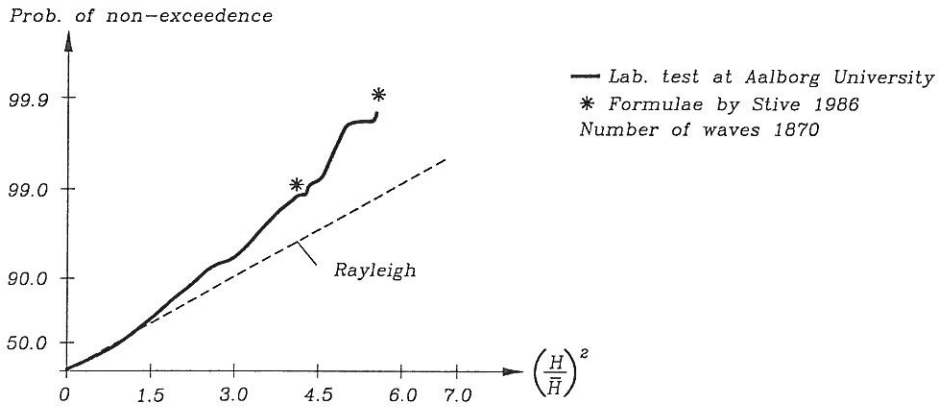

Fig. 4. Comparison of shallow water wave height distribution in Aalborg University test with Dutch prototype data by Stive, 1986.

Analyses performed by CEDEX of some Waverider records of 40 minutes from the location at the bay entrance in 30 metres water depth showed an average ratio of H_{max}/H_s of 1.57 for sea states up to $H_s = 6.5$ m. This is somewhat smaller than the ratio of app. 1.65 valid for the Rayleigh distributed wave heights if we assume app. 200 - 400 waves in the records. For larger sea states no information is available, but even smaller ratios of H_{max}/H_s are expected.

Core material

The core material applied in the AU models was a coarse quartz sand with diameter $D_{50} \simeq$ 2-3 mm. This compares to a rather impermeable prototype core material and is regarded a reasonable modelling of a quarry run core.

Placement of model armour units

Because the method of placement of armour blocks affects the hydraulic stability several different methods of placement were used for the main armour:

- Random placement :
  Several blocks placed in one operation being dumped by hand and smoothed out by hand to meet the requirements for laying density and surface profile. Total randomness ensured.
- Careful random placement :
  Each block was placed by hand in such a way that each block rested against the neighbours, but the pattern was random with no preference orientation.

- Pattern placement by crane, random orientation :
  Each block was placed using a device simulating a crane operation with placement according to prespecified x, y, z-coordinates but allowing random orientation of the blocks.

- Pattern placement by hand or crane, specific orientation :
  Each block was placed by hand in a specific succession in certain positions and oriented with the square side of the block facing the sea. Studies of pattern placements using a model crane were performed by CEDEX and the Port Authority of Bilbao. The final placement pattern is shown in Fig. 5.

For the 100 t units the average number of blocks placed within a unit area of the slope is $N_a = 0.103$ blocks/m^2 independent of the method of placement. The related packing density is $\varphi_n = N_a(\text{block volume})^{2/3} = 1.27$.

The secondary armour blocks were placed randomly in all the tests.

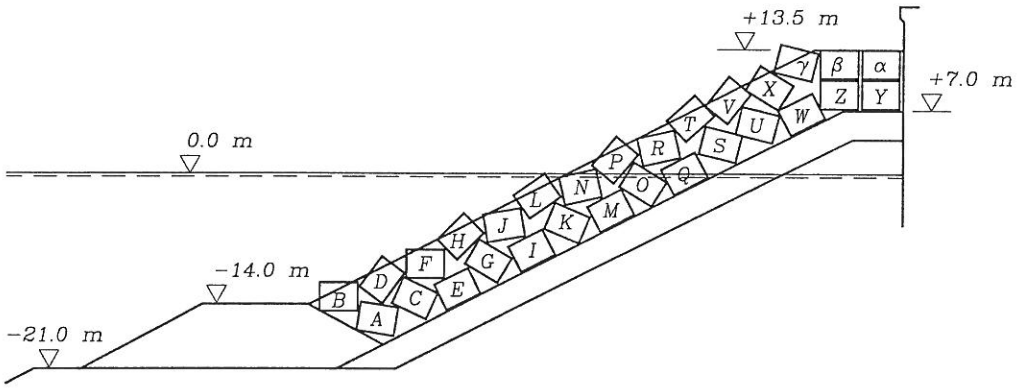

Fig. 5. Final placement pattern for the 100 t parallelepiped blocks. A, B, C, etc. indicate the order in which the blocks are placed.

Registration of armour unit movements

Photos were taken from a fixed position of the complete armoured slope before and after each step in the wave load history. Video recordings of all tests were made. The damage level D is defined as the proportion of blocks displaced more than one block length from their original position. It is also given as N_{od} defined as the number of displaced blocks within a strip of width $D_n = (\text{block volume})^{1/3}$.

Measurement of overtopping water

Mean overtopping discharge was studied by catching the water in trays arranged behind the wave wall. Along trunk sections in the AU tests five trays were arranged behind each other for the determination of the spatial distribution of overtopping water. This was not possible for the corner tests due to the obvious limited space.

Measurement of forces on the wave wall

In the AU tests the horizontal and vertical forces acting on a 25.2 m long wave wall

section were recorded by means of specially designed transducers (strain gauge mounted aluminium beams). Moreover, 5 pressure transducers were arranged in a vertical line with the purpose of providing a check on the recorded total horizontal forces. In order to obtain estimates on the wave generated uplift forces acting on the base of the superstructure a pressure transducer was placed at the lower edge of the wave wall (level +1.5 m). The max uplift force was then calculated in a conservative way using a straight pressure distribution. The existence of a berm of armour blocks resting against the wave wall constitutes a special problem when strain gauge based transducers are used for recording of wave wall forces. This is because the wave forces cause the instrumented wall section to move slightly which can cause wedging of the armour blocks against the wall, thus resulting in changes (drift) in the force signal which are not present in prototype conditions. The drift and the introduced error can be considerable. Pressure transducer recordings avoid this problem, but on the other hand they do not include the real situation where the armour blocks transfer some static (soil mechanic) loads and some wave induced loads to the wall. In the AU experiments the various load components were studied separately and then added together to obtain the total load.

In the CEDEX tests the horizontal load over a 15 m wide wall section was recorded by a strain gauge mounted force transducer.

MODEL TEST RESULTS

Model cross sections

The cross sections referred to in this paper are shown in Fig. 6. They are denoted M1, M2, M3, M6 and M7 for the Aalborg University tests and IIC/IID for the CEDEX tests.

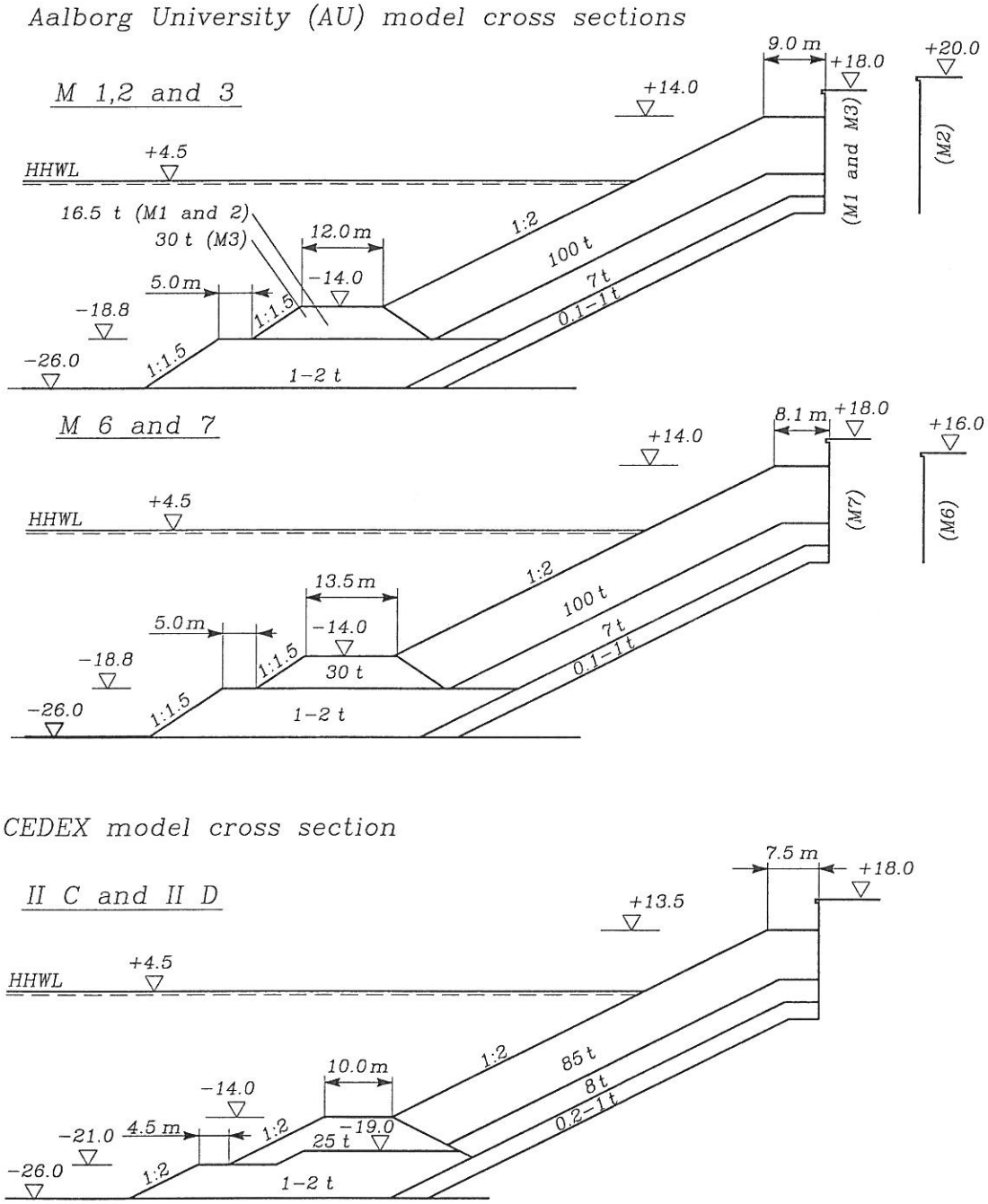

Fig. 6. Model cross sections applied by Hydraulics Laboratory, Aalborg University (AU) and CEDEX.

Main armour stability

Fig. 7 shows the damage as function of H_s for a trunk section armoured with 100 t block exposed to head-on waves. In the Aalborg University tests two different wave wall crest levels of +18.0 m and +20.0 m are presented. However, no clear influence of this difference on the stability is seen, although it would be expected that the higher wall would produce more instability at severe sea states because of the larger reflection of waves. On the other hand a difference of 4.5 m in the still water level is seen to have a clear influence on the stability, surely because of the reduced wave breaking and the larger wave reflection from the wave wall at higher water levels.

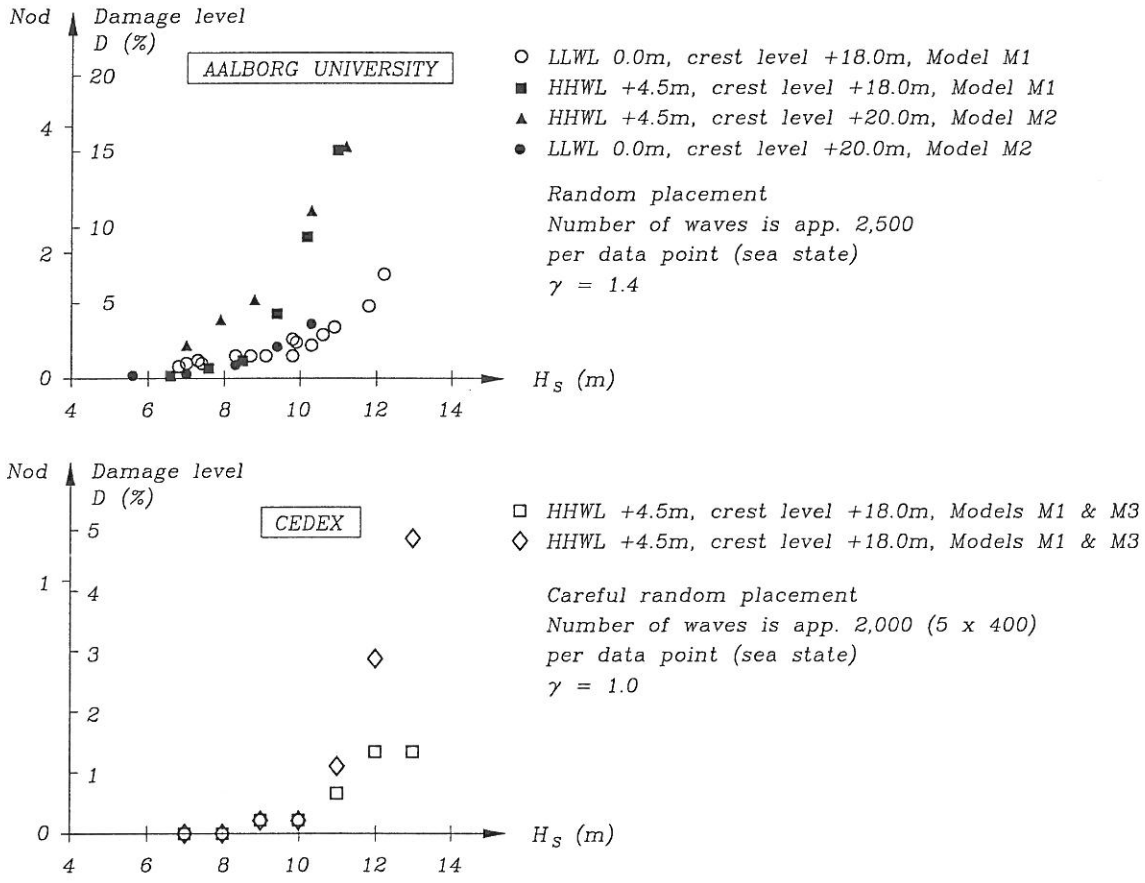

Fig. 7. Hydraulic stability of 100 t parallelepiped blocks in trunk section exposed to head-on waves. Hydraulics Laboratory, Aalborg University and CEDEX, Madrid.

The CEDEX tests show better stability of the armour layer than the AU tests. The difference cannot be explained solely by the more careful placement of the blocks in the CEDEX tests. The fairly large differences in the CEDEX tests result for the large wave heights represents usual scatter for such repeated tests.

The main armour stability in the bend of the outer breakwater is shown in Fig. 8. A very clear difference between the stability in the corner section B and the adjacent sections A and C cannot be seen, although there is a tendency that for the more severe sea states

the damage is less in the corner than in the two adjacent sections.

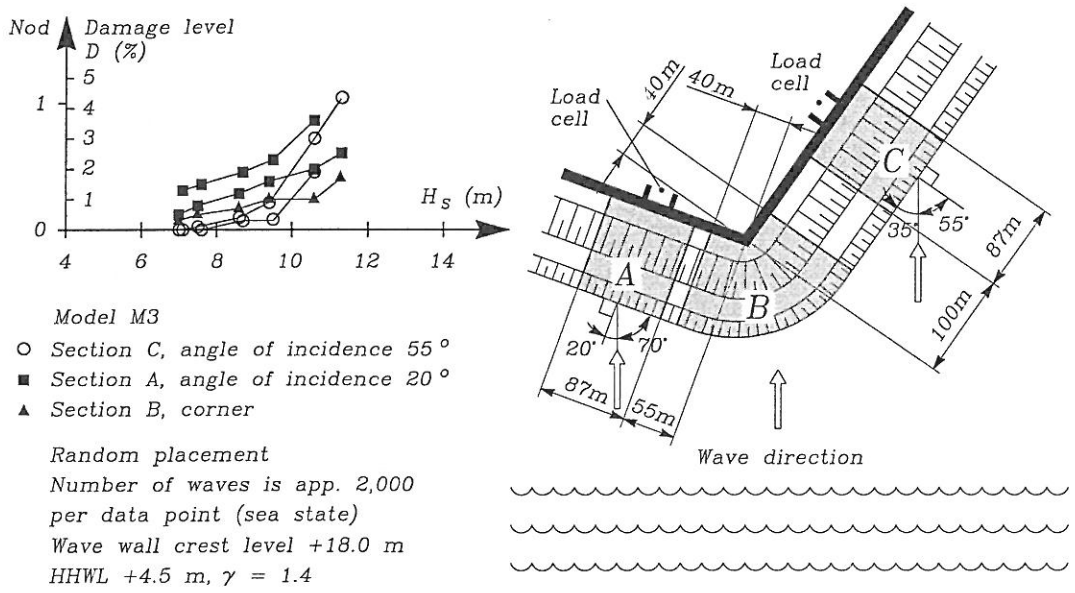

Fig. 8. Hydraulic stability of 100 t parallelepiped blocks in the corner and the two adjacent sections exposed to oblique waves. Hydraulics Laboratory, Aalborg University.

The influence of the method of block placement is shown in Fig. 9 for the section A (Fig. 8), exposed to waves with a 20 degree angle of incidence. The applied methods of placement is described earlier.

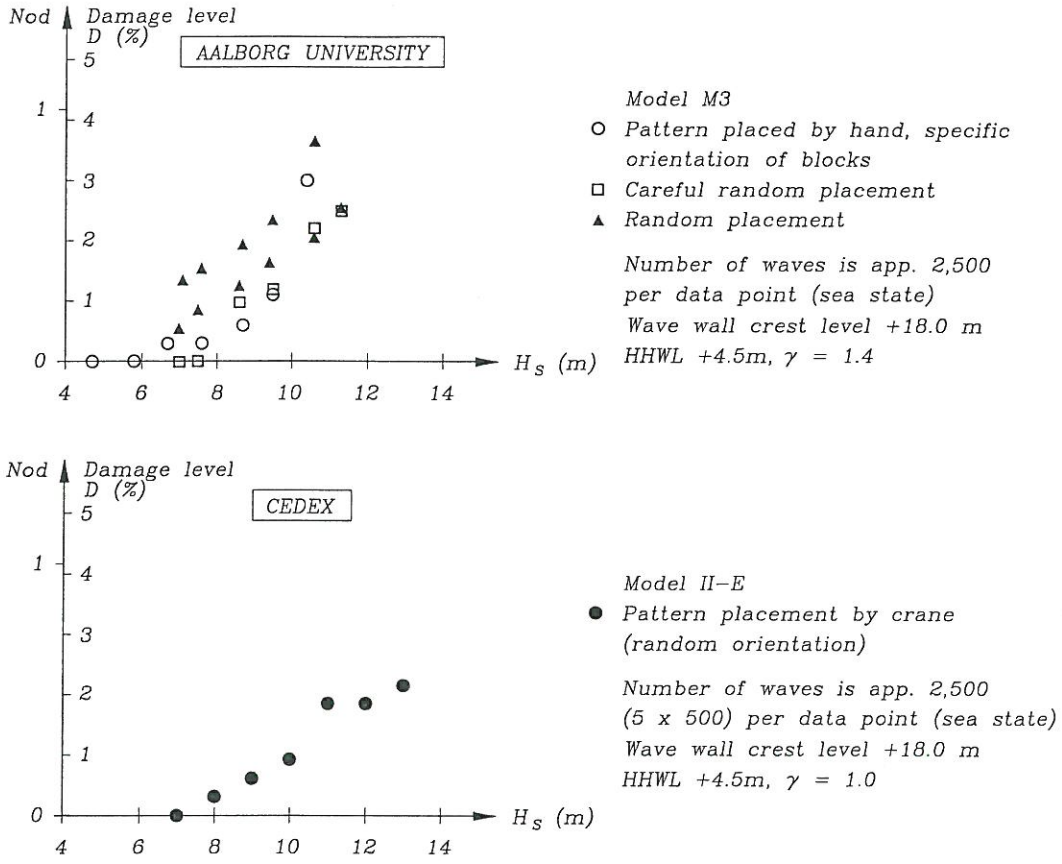

Fig. 9. Influence of method of block placement on the hydraulic stability of 100 t parallelepiped blocks. Angle of incidence of the waves is 20 degrees. Hydraulics Laboratory, Aalborg University and CEDEX, Madrid.

It is seen from the Aalborg University tests that, as expected, the more careful placement gives better stability for the milder sea states, but for the severe sea states there is little difference in the stability. The agreement with the tests of CEDEX is good.

The influence of angle of incidence of the waves on the main armour stability in the trunk sections is shown in Fig. 10.

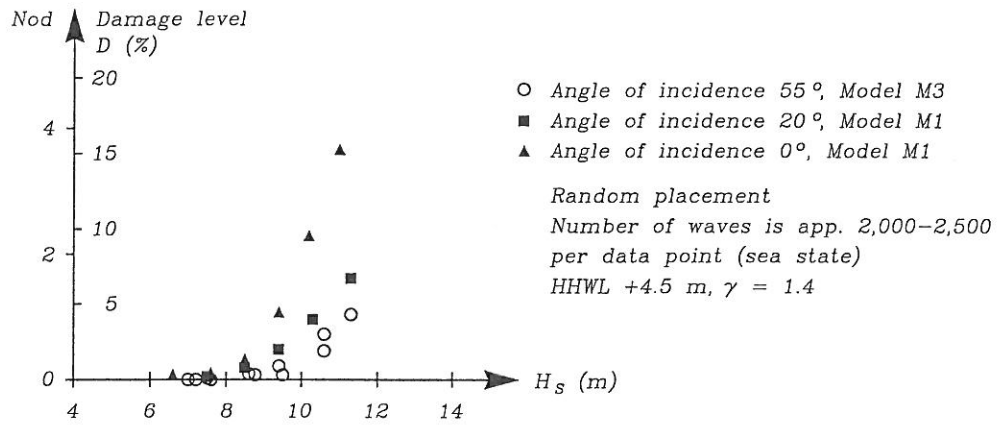

Fig. 10. Influence of the angle of incidence of the waves on the hydraulic stability of 100 t parallelepiped blocks. Hydraulics Laboratory, Aalborg University.

Fig. 11 shows the influence of block size on the hydraulic stability of the main armour in the corner section B (Fig. 8).

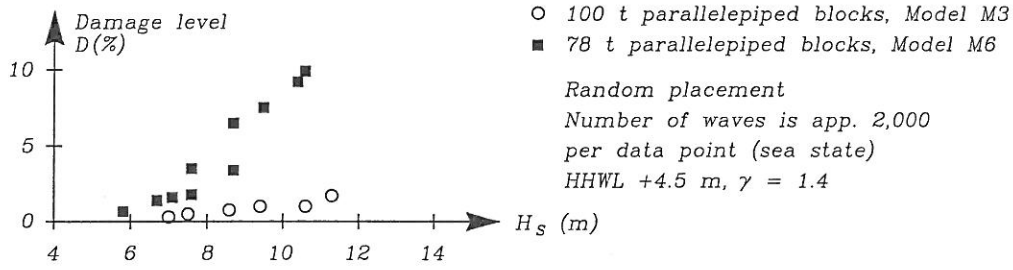

Fig. 11. Influence of the block size on the hydraulic stability of the main armour in the corner section B (see fig. 8). Hydraulics Laboratory, Aalborg University.

The berm stability

The stability of the toe berm armoured with 16.5 t parallelepiped blocks are shown in Figs. 11 for high and low water conditions. For each water level is represented two sets of results corresponding to wave wall crest levels of +18.0 m and +20.0 m. In the Figures is also shown the formula by Gerding (1993) valid for berms armoured with rock at the toe of a rock armoured straight non-overtopped slope, 1 : 1.5.

$$\frac{H_s}{\Delta D_{n50}} = \left(0.24\,\frac{h_t}{D_{n50}} + 1.6\right) N_{od}^{0.15} \qquad \text{(Gerding, 1993)} \qquad (1)$$

where $\Delta = \dfrac{\text{density of armour}}{\text{density of water}} - 1$, D_{n50} is equivalent cube length and h_t is the water depth over the toe berm.

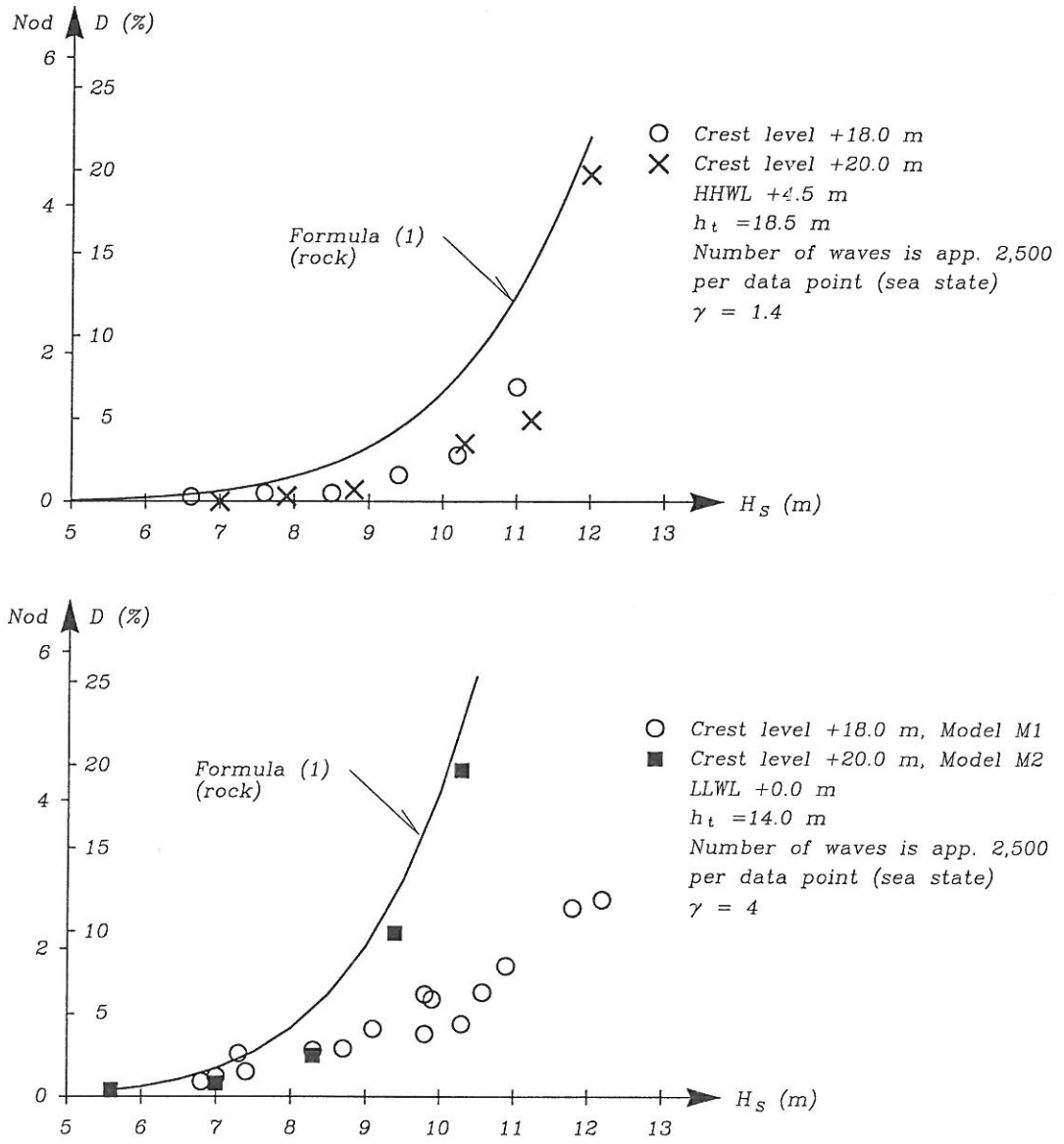

Fig. 12. Hydraulic stability of the toe berm armoured with 16.5 t randomly placed parallelepiped blocks. Hydraulics Laboratory, Aalborg University.

It is seen that the stability of the parallelepiped blocks is better than predicted by formula (1). This is to be expected because the formula is based on model tests with rock as berm armour and a steeper slope of 1 : 1.5 for the main armour.

Wave forces on parapet wall

Figs. 13, 14 and 15 show for the case of angle of wave incidence of 20 degrees the recorded horizontal forces on the wave wall and the wave generated pressure at the foot of the wall in level +1.5 m. The latter is used for the calculation of the wave generated lift forces on the super structure. The tests at AU showed very good agreement between the wave recorded by the strain gauge transducers and the pressure transducers.

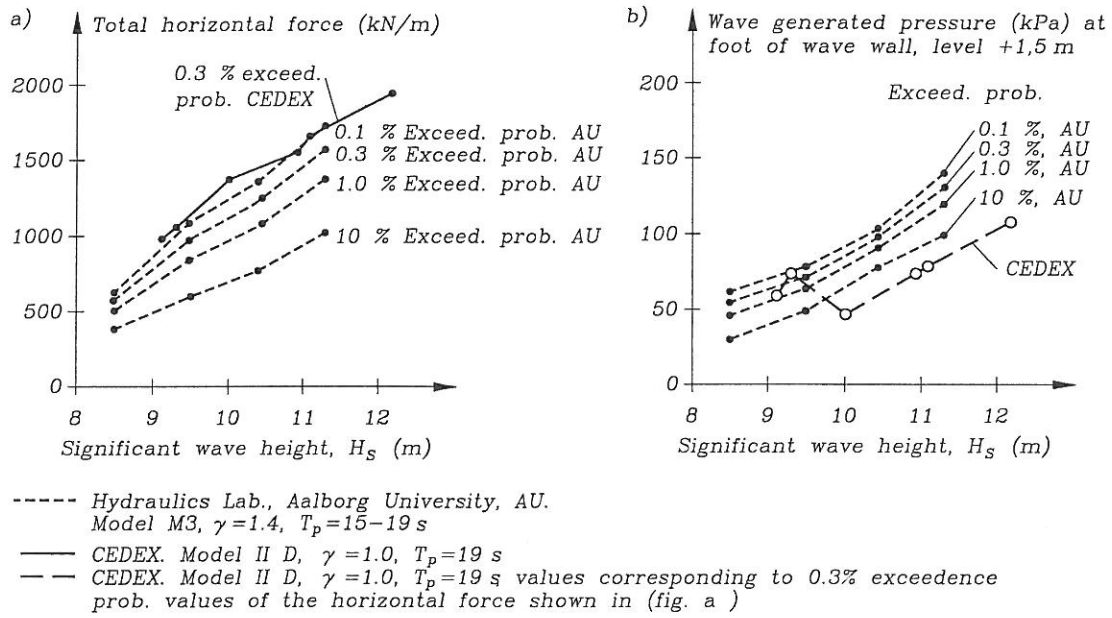

Fig. 13. Exceedence probability levels of total horizontal force (wave generated + hydrostatic force for SWL = +4.5 m + force from armour units) on wave wall and wave generated pressure at foot of wall. The hydrostatic force is 45 KN/m. Angle of incidence of waves 20 degrees. Hydraulics Laboratory, Aalborg University (Model M3) and CEDEX, Madrid. (Model IID).

The differences in recorded horizontal forces of app. 10-15% between the AU and the CEDEX tests might, at least to some extent, be explained by the differences between the applied models, cf. Fig. 6. However, the differences related to the pressure at level +1.5 m seem to be surprisingly large for the larger H_s-values.

The recorded wave generated pressure at the foot of the wave wall is shown in Fig. 14. In the same Figure is shown an example of the correlation between this pressure and the wave generated horizontal force.

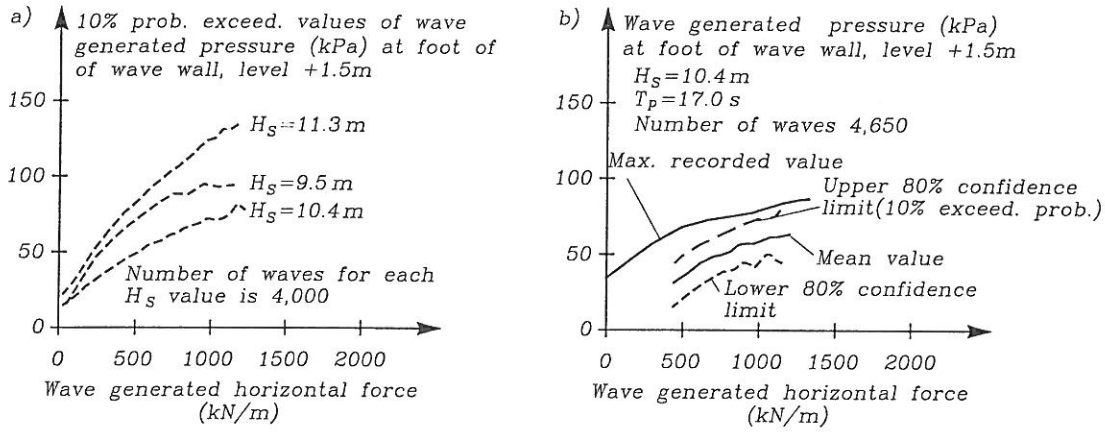

Fig. 14. Wave generated pressure at level +1.5 m at the foot of wave wall with crest level +18.0 m. HHWL +4.5 m, γ = 1.4. Wave direction 20 degrees angle of incidence. Hydraulics Laboratory, Aalborg University. (Model M3).

Fig. 15 shows the mean values of the level of the wave generated horizontal force resultant as well as an example of the correlation between this level and the wave generated horizontal force.

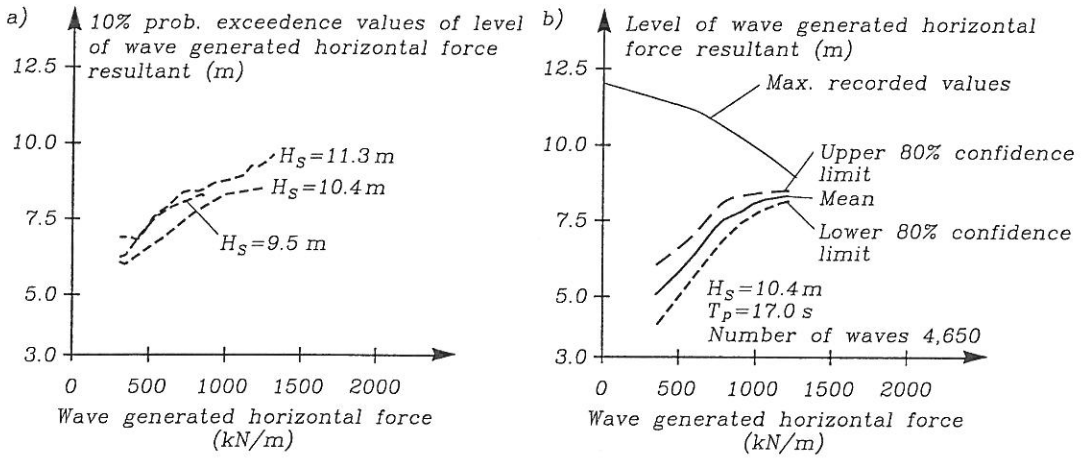

Fig. 15. Level of resultant of wave generated horizontal force at wave wall. HHWL +4.5 m. γ = 1.4. Wave direction 20 degrees angle of incidence. Hydraulics Laboratory, Aalborg University. (Model M3).

The level of the resultant of the 0.3% exceedence probability horizontal force found in the CEDEX tests (model IID) is shown in Fig. 16.

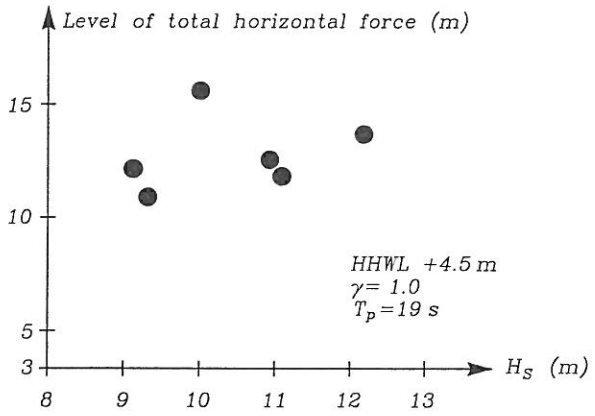

Fig. 16. Level of total horizontal force resultant corresponding to the 0.3% exceedence probability horizontal force values. Wave direction 20 degree angle of incidence. CEDEX, Madrid. (Model IID).

The levels of the resultant seem very high compared to the results of AU shown in Fig. 15. The latter are supported by recorded pressure distributions, cf. Fig. 17, which shows typical examples for breaking and non-breaking waves.

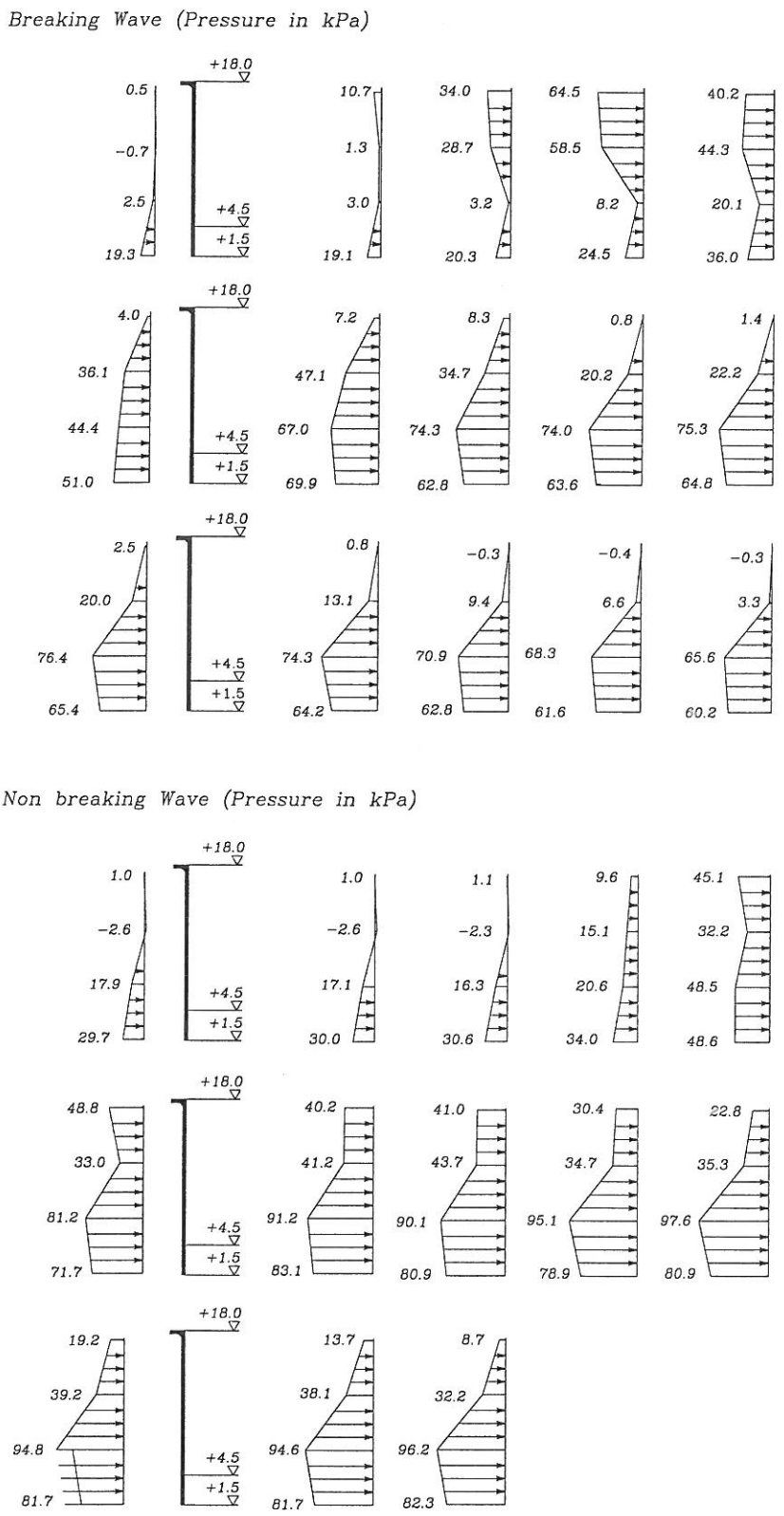

Fig. 17. Typical wave generated pressures on the wave wall. HHWL +4.5 m, H_s = 10.4 m, T_p = 17.0 s, γ = 1.4. Time lag between the shown recordings are 0.37 s. 20 degree angle of incidence of the waves. Hydraulics Laboratory, Aalborg University. (Model M3).

Uplift force on wave wall nose

In the Aalborg University tests the statistics of the wave generated uplift (vertical) force on the one meter wide protruding nose of the wave wall was recorded as well as the correlation with the horizontal wave generated force. The vertical force was found to be app. 5-7% of the horizontal force for the larger sea states, i.e. H_s = 10-11 m.

Overtopping

The significant influence of the water level on overtopping is shown in Fig. 18 together with a comparison with values predicted by the formula by Bradbury et al. (1988) using the coefficients corresponding to the closest geometrical fit of the cross section.

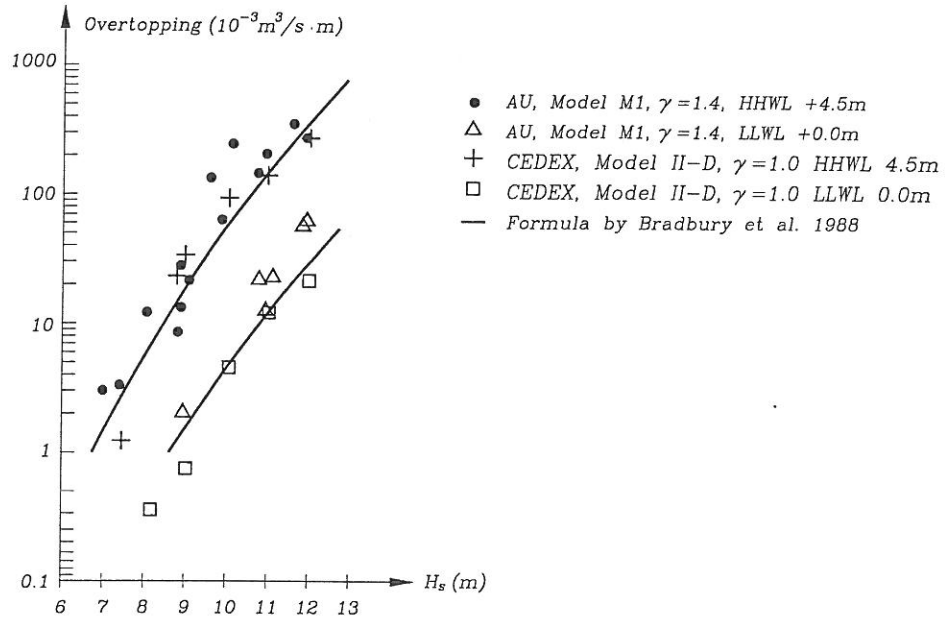

Fig. 18. Recorded overtopping for head-on waves and comparison with the formula by Bradbury et al. (1988). Hydraulics Laboratory, Aalborg University and CEDEX, Madrid.

It is seen that there is good agreement between the results from the two laboratories. The formula by Bradbury seems also to be in fair agreement with the test result when it is considered that the involved geometries are not identical.

The influence of the angle of incidence of the waves is shown in Fig. 19.

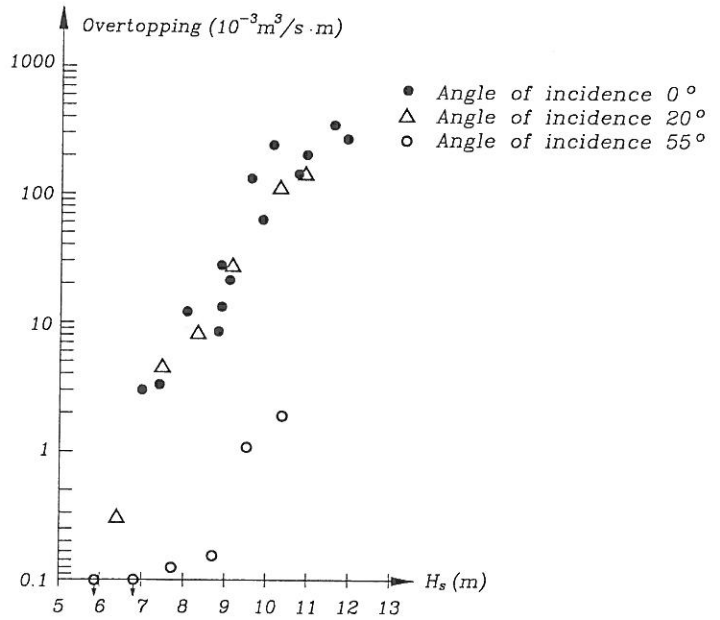

Fig. 19. Example of the influence of the angle of incidence of the waves on the overtopping. HHWL +4.5 m. Model M 1. Hydraulics Laboratory, Aalborg University.

The distribution of the downfall of overtopping water in the area behind the wave wall depends on the amount of overtopping water, on the wave period, on the spectral peak enhancement factor and on the wave wall crest level. Fig. 20 shows for head-on waves the relative spatial distributions behind the wall for some of these factors. The area under each curve corresponds to 100% discharge of overtopping water.

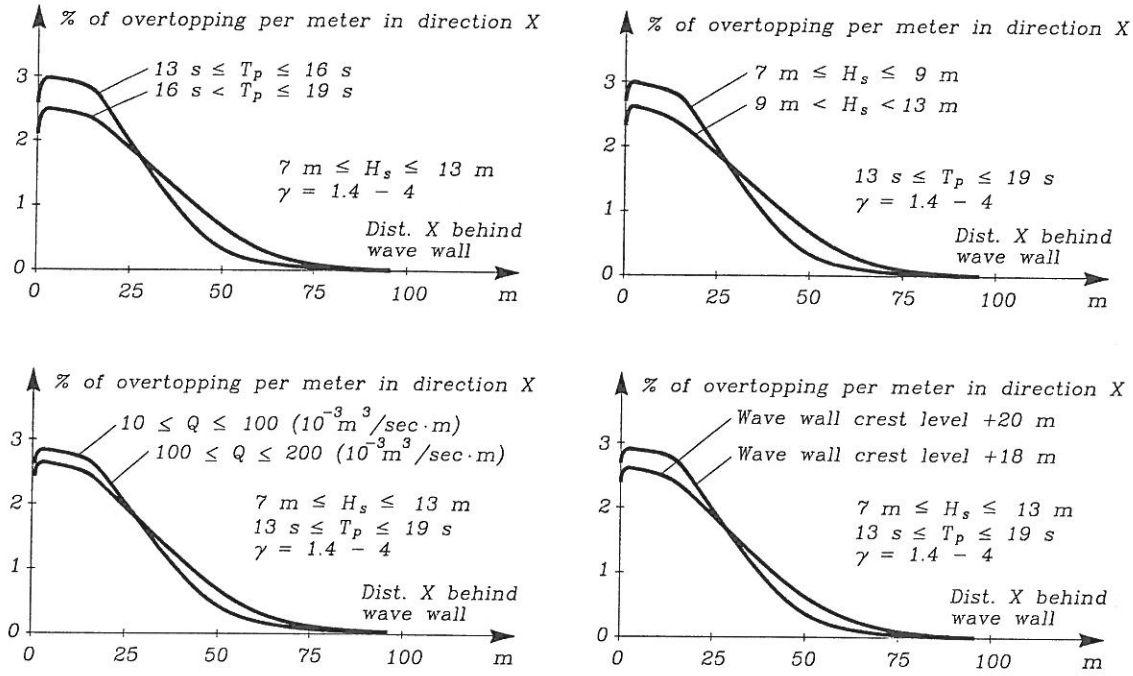

Fig. 20. Relative spatial distribution of mean values of overtopping water behind the wave wall. Head-on waves. HHWL +4.5 m. Model M1 and M2. Hydraulics Laboratory, Aalborg University.

Stability analysis of wave wall

The stability analysis was performed by the design office of the Port Authority of Bilbao and University of Barcelona using the computer programs STABL by University of Purdue. Together with the overall slope stability analyses, mentioned below, more than 10,000 different sliding surfaces were tested. Dynamic effects were disregarded.

The massive concrete superstructure is shown in Fig. 3 for the largest cross sections. Two failure modes of the wall section were considered: horizontal displacement (sliding) and tilting (due to ground failure). Formation of a crack between the massive wall and the two metre thick slap is foreseen and accepted. The wave generated uplift force was assumed linearly distributed with max value at the front corner of the wave wall toe and a zero-value at the rear of the slab.

For the sliding analysis a friction coefficient of 0.8 was used. This value is commonly used in the design of dam structures and is larger than the value of 0.6, which was found in earlier static prototype tests for the investigation of the friction between concrete slabs

and rock material. These tests were performed during the construction of the Punta Lucero Breakwater. The reason for applying the higher value of the friction coefficient is that the failure surface will cut through the core material due to the deep toe of the wall, cf. Fig. 3.

The minimum applied safety factor was 1.2.

The design of the wave wall is prepared for an increase in height due to possible future wishes for reduced overtopping.

FOUNDATION OF THE BREAKWATER

Geotechnical site investigations

The purpose of the investigation was to obtain soil mechanics information which would allow evaluation of:

- penetration of construction material into the sea bed
- settlement of the sea bed due to the weight of the structure
- overall and local stability of the structure under wave loading
- stability of the sea bed under wave loading

The investigations were carried out by the Port Authority of Bilbao under the supervision of University of Barcelona. The main contractor was Fugro - McClelland. The site investigations consisted of

- sidescan and sub-bottom profiling
- vibrocoring
- 11 wash boring and rotary coring to depths between 2 and 35 metres
- 39 quasi-static piezocone penetration tests to depths between 1 and 26 metres

The investigations revealed fairly favourable foundation conditions of approximately 25 metres of loose to dense, fine to medium sands overlaying a mudstone. However, in some areas was discovered 1 to 3 metres thick layers of loose silt located approxemately 3 metres below the sea bed.

Main results of analyses of stability and settlements

Stability analyses showed that because of the weakness and the proneness to liquefaction of the loose silt layers it was necessary to remove part of the silt layer by dredging two 50 metres wide trenches to be filled with core material on each side of the breakwater. The most dangerous failure surfaces and the related stability ratios (safety coefficients)

are shown in Fig. 21 for the cases with and without the dredged tracks. The failure surfaces always pass through the silt layer. The effect of the downrush was considered in the analysis.

An additional geotechnical investigation has been carried out during the works and has shown that the main characteristics of the soft silt layer was much better than previous considered in the project. Consequently new solutions are being investigated.

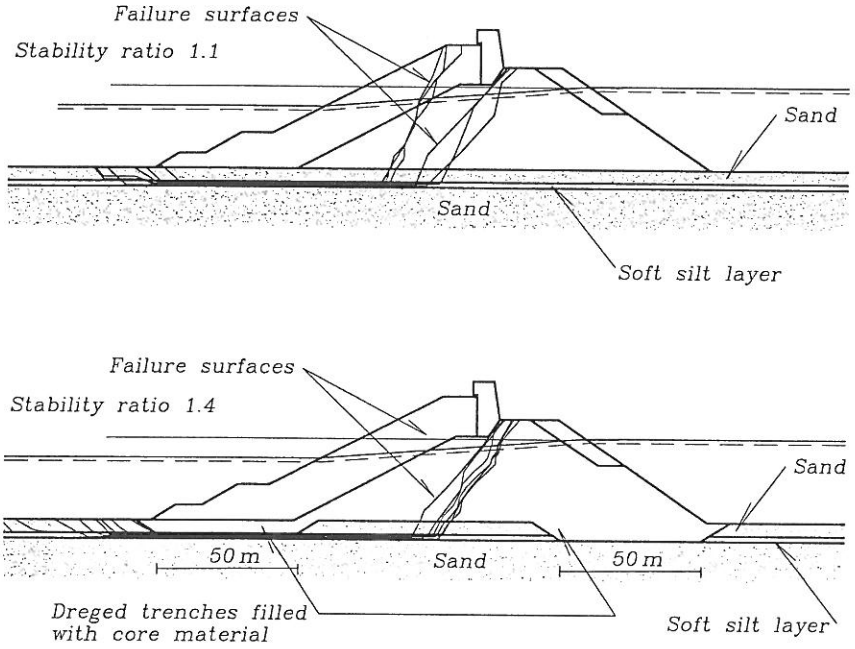

Fig. 21. The most dangerous failure surfaces for cross sections with and without dredged trenches filled with core material.

The settlement analyses predict that at the end of the construction period the total settlement (instant) of the foundation soils will be in the order of 40 to 50 cm. The total instant settlement of the breakwater itself is estimated to be 11 to 15 cm. The corresponding figures for total settlement over a 18 years period are 7.5 cm and 8 - 38 cm, respectively.

REFERENCES

Ciervana Breakwater. Puerto Autonome de Bilbao. Model Test Report, Oct. 1., 1992. Hydraulics Laboratory, Aalborg University, Denmark.

Ensayos para la medida de esfuerzos y rebases en el dique de Ciervana. Informe Final, April 1990. CEDEX, Madrid, Spain.

Stive, M.J.F., 1986. Extreme shallow water wave conditions. Delft Hydraulics. Internal report H533.

Gerding, E., 1993. Toe structure stability of rubble mound breakwaters. Masters thesis at Delft University of Technology, The Netherlands, 1993.

Bradbury, A.P., Allsop, N.W.H., 1988. Hydraulic effects of breakwater crown walls. Proc. Conf. Breakwater '88, Eastbourne, Institution of Civil Engineers, U.K.